An Adaptive High-gain Observer for Wastewater Treatment Systems

Frederic Lafont[a,*], Eric Busvelle[b], Jean-Paul Gauthier[a]

[a] *Universite du Sud-Toulon-Var, LSIS, UMR CNRS 6168, B.P 20132, 83957 La Garde Cedex, France*
[b] *IUT Dijon-Auxerre, LE2I, UMR CNRS 5158, Route des plaines de l'Yonne, 89000 Auxerre, France*

Abstract

The purpose of this paper is twofold: 1. We apply the adaptive observer developed in Boizot et al. (2010) to a wastewater system, following two cascade steps. First, we apply it to a simplified model of the system. Second, we use this "simplified" estimation as a measurement for the full system. 2. Although the observability analysis is trivial, the equations contain rather complicated terms. Therefore, it is not reasonable to change coordinates for those of the required observability canonical form. Hence, we have to establish and work with the "unusual" equations of the observer in natural coordinates.

Let us point out that the simulations are done taking into account the small number of measurements (three) available in practice.

Keywords: Nonlinear observer and filter design, Wastewater treatment processes

*Corresponding author: lafont@univ-tln.fr
Tel.: +33(0)494142078

1. Introduction

The present work deals with the observer design of non linear dynamical systems, and application to a wastewater treatment system.

The need to develop observers or "software sensors" for Activated Sludge Processes in perspective of on-line monitoring is due to the following facts, among others:

1) Although sensors for measuring chemical and biological variables are widespread and very advanced, such measurements are still unreliable and noisy,

2) The implementation and maintenance costs of these adavanced sensors are high.

A lot of work has been developed on the synthesis of nonlinear observers for (bio)chemical processes (Alcaraz-Gonzalez et al., 2002; Assis and Filho, 2000; Bastin and Dochain, 1990; Bastin and Impe, 1995; Busvelle and Gauthier, 2003, 2005; Chachuat et al., 2003; Dochain, 2008; Gauthier et al., 1992; Nejjari et al., 2008; Rapaport and Dochain, 2005; Sotomayor et al., 2002). Here, we have chosen an adaptive high-gain observer as proposed in the paper (Boizot et al., 2010) for the following reasons. This observer is high-gain, but it is also extended-Kalman-filter based: First, in the context of large transitions, it is an high-gain (HG) observer which guarantees theoretical convergence with arbitrary rate, under certain observability assumptions. Second, for small enough initial estimation error, it behaves like a classical extended Kalman filter (EKF), i.e. it is more or less optimal w.r.t. noise. Moreover, in a deterministic setting, it has good convergence properties (Baras et al.,

1988).

Here, transition from HG mode to EKF mode is performed via an adaptation procedure based upon the level of innovation (i.e. the level of new information appearing through the "recent" observations).

For the general theory of high-gain nonlinear observers, (see Boizot and Busvelle, 2007; Boizot et al., 2010; Busvelle and Gauthier, 2005; Gauthier and Kupka, 2001).

The EKF is widely used and works rather well in practice. The main disadvantage for the EKF algorithm is that it requires an approximate knowledge of the initials conditions. Conversely, the HG-EKF algorithm converges whatever the initial guess but is rather sensitive with respect to noise. Then, the idea is to switch between the EKF and the HG-EKF algorithm. If the estimation error of the HG-EKF becomes sufficiently small then the EKF is used. The switching between these two modes can be done by having the high-gain parameter θ evolving between 1 and θ_{max}. The adaptation is made by using a differential equation driven by the "innovation".

Usually this method is applied by previously changing coordinates in order to put the system under a certain observability canonical form. In our case, we prefer to write our observer in the natural coordinates in order that it is not necessary to realize on-line the inverse coordinates change. The counterpart of this choice is that the Riccati equation of the Kalman filter has not the standard form. Detailed computations are provided in our appendix A.

Moreover here, in order to simplify the computations, we use cascade observers (reduced and complete): A first observer of the type above is used on a simplified model to provide an intermediate estimate of the state, this

estimation being itself used as the output of the non simplified system. Actually, for the complete observer with the three practical outputs, the computations are very heavy, even working in natural coordinates.

In Section 2 we recall the structure of our observer, which is just the multi-output version of the one developed in the paper (Boizot et al., 2010). The section 3 is devoted to the crucial concept of innovation, which is used in order to switch between the EKF and HG-EKF modes. The section 4 presents in a few lines the idea of a cascade observer. Section 5 is devoted to the application to a wastewater treatment plant. First we recall the equations of the process, in full and simplified form. Then we perform the observability analysis in both cases. Thirdly we show noisy simulation results for the cascade observer.

2. Systems under consideration and observer equations

2.1. The observability canonical form

We consider a smooth nonlinear system of the form:

$$\begin{aligned} \tfrac{dx}{dt} &= f\left(x,u\right), \\ y &= h(x) = Cx, \end{aligned} \tag{1}$$

which is mapped by a diffeomorphism ψ into the following system:

$$\begin{aligned} \tfrac{d\xi}{dt} &= F\left(\xi,u\right) = A\left(t\right)\xi + b\left(\xi,u\right), \\ y &= C\xi, \end{aligned} \tag{2}$$

where $x,\ \xi \in \mathbb{R}^n$ are the state vectors, where u, the control variable belongs to a certain bounded subset of $\mathbb{R}^p$ and the output $y \in \mathbb{R}^{d_0}$.

Note: We have chosen to consider a linear output only, since it corresponds to our practical case and computations are simpler. However the general case is similar.

The matrices $A(t),\ C$ and the vector $b\left(\xi,u\right)$ have a following form:

$$A(t)=\begin{pmatrix}0 & a_2(t) & 0 & \cdots & 0\\ 0 & 0 & a_3(t) & \ddots & \vdots\\ \vdots & \cdots & \ddots & \ddots & 0\\ \vdots & \cdots & \cdots & 0 & a_k(t)\\ 0 & 0 & \cdots & \cdots & 0\end{pmatrix}, \tag{3}$$
$$C=(a_1(t),0,\cdots,0)=(Id,0,\cdots,0),$$

where Id is the d_0 identity matrix.

$$b(\xi,u)=\begin{pmatrix}b_1(\xi_1,u)\\ b_2(\xi_1,\xi_2,u)\\ \vdots\\ b_n(\xi_1,\cdots,\xi_n,u)\end{pmatrix}. \tag{4}$$

The state vector $\xi(t)$ is assumed to have a "block" structure $\xi=\left(\xi_1^{'}\ \xi_2^{'}\ \cdots\ \xi_n^{'}\right)^{'}$, where $\xi_i\in\mathbb{R}^{d_i}$ with $d_0\geq d_1\geq\cdots\geq d_k$. The matrices $a_i\left(t\right)$ have dimension $d_{i-1}\times d_i$ and belong to a compact subset K_i of the set of $d_{i-1}\times d_i$ matrices of maximum rank d_i. The $f\left(x,u\right),\ a_i\left(t\right),b_i\left(\xi,u\right)$ are assumed smooth w.r.t ξ, u and t, the b_i depend on ξ in a "block" triangular way and are compactly supported.

Along the paper x (resp. ξ) is called the **natural** coordinate (resp. the

observable coordinate).

The structure conditions guarantee obviously "uniform" and "uniform infinitesimal" observability in the sense of Gauthier and Kupka (2001). The compact support conditions can be artificially forced outside the "practical" domain where the state is assumed to remain. All the results in Boizot et al. (2010) extend without any difficulty to the case of such a structure with such "compact support" assumptions. It is just a matter of rewriting.

It follows from the observability theory in Gauthier and Kupka (2001) that this canonical form together with the associated regularity assumptions is pertinent in several situations: For any system meeting strong observability assumptions, coordinates can be changed for "observable coordinates" in which this canonical form is met.

Along the paper TF denotes the tangent mapping to the mapping $F : x \to F(x)$, $\mathbb{R}^n \to \mathbb{R}^n$ i.e. its Jacobian matrix in coordinates. Accordingly T^2F denotes the double tangent, a skew-symmetric bilinear mapping, $\mathbb{R}^n$-valued, and for any $u \in \mathbb{R}^n$ we define the matrix $D^2F(x)\{u\}$ by $T^2F(u,v) = D^2F(x)\{u\} \cdot v$.

We denote by L_b the bound on the Jacobian matrix $Tb(\xi,u)$ of $b(\xi,u)$ (i.e. $\|Tb(\xi,u)\| \leq L_b$). Since $b(\xi,u)$ is compactly supported and u is bounded, b is Lipschitz w.r.t ξ uniformly in u: $\|b(\xi,u) - b(\eta,u)\| \leq L_b \|\xi - \eta\|$.

2.2. Observer structure in observable coordinates

Let Q $(n \times n)$, R $(d_0 \times d_0)$ be symmetric positive definite matrices. Let θ be the high-gain parameter, $\theta \geq 1$. For $\theta = 1$ the observer will just be an ordinary EKF.

Set $\Delta = BD\left(1, \frac{1}{\theta}, \cdots, \frac{1}{\theta^{k-1}}\right)$, the block diagonal matrix with diagonal blocks

$Id_{d_0}, \frac{1}{\theta} Id_{d_1}, \cdots$. Set $Q_\theta = \theta \Delta^{-1} Q \Delta^{-1}, R_\theta = \theta^{-1} R$. The equations of the system in observable coordinates are:

$$\begin{array}{l} \frac{d\xi}{dt} = T\psi\left(\psi^{-1}(\xi)\right) f\left(\psi^{-1}(\xi), u\right), \\ \frac{d\xi}{dt} = F\left(\xi, u\right). \end{array} \tag{5}$$

$$y = C\xi. \tag{6}$$

The equations for the HG-EKF in the observable coordinates are:

$$\frac{d\hat{\xi}}{dt} = F(\hat{\xi}, u) + PC' R_\theta^{-1}(y - C\hat{\xi}), \tag{7}$$

$$\frac{dP}{dt} = TF(\hat{\xi}, u)\ P + P\ TF(\hat{\xi}, u)' + Q_\theta - PC' R_\theta^{-1} CP. \tag{8}$$

In the natural coordinates we have $\hat{x} = \psi^{-1}(\hat{\xi}) = \Phi\left(\hat{\xi}\right)$, where $\hat{x}$ denotes the estimate of x. Following our appendix A, the equations for the HG-EKF become:

$$\frac{d\hat{x}}{dt} = f(\hat{x}, u) + pC'\left(\hat{x}, u\right) R_\theta^{-1}\left(y - h\left(\hat{x}\right)\right), \tag{9}$$

$$\begin{array}{l} \frac{dp}{dt} = Tf(\hat{x}, u)p + pTf(\hat{x}, u)' + q_\theta(\hat{x}) - pC' R_\theta^{-1} Cp \\ +T\psi(\hat{x})^{-1} D^2\psi(\hat{x}) \left\{pC' R_\theta^{-1}\left(h(\hat{x}) - y\right)\right\} p \\ +pD^2\psi(\hat{x}) \left\{pC' R_\theta^{-1}\left(h(\hat{x}) - y\right)\right\}' \left(T\psi(\hat{x})^{-1}\right)', \end{array} \tag{10}$$

where

$$q_\theta\left(\hat{x}\right) = \left(T\psi\left(\hat{x}\right)\right)^{-1} Q_\theta \left(\left(T\psi\left(\hat{x}\right)\right)^{-1}\right)'. \tag{11}$$

3. Innovation

The function In_d introduced below and called the innovation reflects the quality measurement of the estimation error on a small moving time interval

of size d. The strategy is to adapt the High-gain parameter θ according to In_d. Due to the observability properties of our system, if the estimate $\hat{x}$ is far from x then θ will increase to High-gain mode. Contrarily, if $\hat{x}$ is close to x, innovation will be small and θ will decrease to 1 (Kalman filtering mode). For this, the variable θ will be subject to the differential equation (15) just below.

Let $G_o(\theta)$ be defined as follows:

$$G_o(\theta) = \begin{cases} \frac{1}{\Delta T}\theta^2 \text{ if } \theta \leq \theta_1, \\ \frac{1}{\Delta T}(\theta - 2\theta_1)^2 \text{ if } \theta > \theta_1, \end{cases} \tag{12}$$

where $\theta_1 = \frac{1}{2}\theta_{max}$ and ΔT small enough is a constant.

The innovation $In_d(t)$, with forgetting horizon d, is:

$$In_d(t) = \int_{t-d}^{t} \|y(\tau) - \hat{y}(\tau)\|^2 d\tau, \tag{13}$$

where $\hat{y}(\tau)$ is the prediction from the initial state $\hat{x}(t-d)$.

Let us define

$$G(\theta, In_d) = \mu(In_d) G_o(\theta) + (1 - \mu(In_d)) \lambda (1 - \theta), \tag{14}$$

for a $\lambda > 0$ and with $\mu(In_d)$ a smooth function equal to 1 if $In_d \geq \gamma_1$, to 0 if $In_d \leq \gamma_0$, with $0 \leq \mu(In_d) \leq 1$ for $\gamma_0 \leq In_d \leq \gamma_1$. Another admissible choice for μ is a sigmoid function, $\mu :]0; +\infty[\rightarrow]0; 1[$, $\mu(In_d) = \frac{1}{1+e^{-\beta \cdot (In_d - m)}}$. The equation for the HG parameter θ is:

$$\dot{\theta} = G(\theta, In_d). \tag{15}$$

The parameters β and m of the sigmoid play the same role as the parameters γ_0 and γ_1. The zero value of the sigmoid function corresponds to "moving

towards Kalman filtering mode" with maximum speed, although the value one corresponds to "moving towards the high gain mode" with maximum speed. The duration of the transition part is controlled by the parameter β (The higher β, the shorter the transition). In practice, the best results are obtained for a small transition time i.e a large value of β. All details can be found in Boizot et al. (2010).

Finally our adaptive observer in original coordinates is given by the set of equations (9, 10, 13, 15).

Comment 1: Roughly speaking, we can summarize the methodology as follows:

1) A single Extended Kalman Filter equation, depending on a single parameter θ realizes the observers in both modes: for $\theta = 1$, it coincides with the ordinary Extended Kalman Filter. For θ large it is a HG-KF, as proposed for instance in Gauthier and Kupka (2001).

2) Guarantee of convergence of the error is obtained (see 4 below) in observable coordinates only. It is possible to overcome the dificulty of performing this coordinate change on-line, via the equations (9, 10, 11) of the transformed EKF equations to natural coordinates.

3) The dynamics of the parameter θ is driven by the "innovation" term computed over a slipping window. Small innovation means that the estimation error is close to zero, hence, it is suitable to move θ to ordinary EKF mode. Conversely, large innovation means large estimation error, hence, the strategy is to move to high-gain mode. This is done via the "driving equation" 15.

4) It is well known that the Riccati matrix P is related to the Gramm observ-

ability matrix of the linearized system along the estimate trajectory. Then it reflects the "innovation" relative to this linearized system. However, this "linearized innovation" is not enough for our purposes.

5) **Guarantee of convergence:** Following Boizot et al. (2010), the convergence result is as follows: For all noise characteristics (Q,R) (depending on the noise in EKF mode) the parameters (θ, m, d, β) can be chosen in such a way that global arbitrary exponential convergence can be achieved: $\|\epsilon\| \leq e^{-\alpha(t-T^*)} \times \|\epsilon_0\|$, ($\alpha$ arbitrary, T^* arbitrary).

Comment 2: Due to (13) the observer system (9, 10, 13, 15) is not a system of ODE. However existence and uniqueness of solutions is guarantied and it is more or less clear how to proceed numerically.

4. The interest of natural coordinates, and of a cascade observer

It turns out that the change of variable $\psi(x)$ is not so easy to apply. It is the reason why we have chosen to work in natural coordinates. In these natural coordinates according to our observer equations, it is enough to be able to compute the inverse Jacobian $D\psi(\hat{x})^{-1}$. For our application below, this would be still hard in the case of the full equations. It is why we have chosen (in natural coordinates) the following strategy.

We apply first our observer to a simplified model (five states, three outputs). We use the estimate provided by this first observer as the output of the full system. In this way the computation of both inverse Jacobians is easy (See Fig. 1).

Insert figure 1 about here

5. Application

The process under consideration is a real small-size wastewater treatment plant composed of a unique aeration tank equipped with surface aerators which provide oxygen and mix the influent wastewater with biomass (Fig. 2). Here, we address the question of online estimation of the effluent quality.

Insert figure 2 about here

A European Union directive fixed the maximum pollutant concentrations allowed in the effluent of small size wastewater treatment plants: The biochemical oxygen demand over an elapsed period of five days $BOD_5 < 25\ mg/l$, the chemical oxygen demand $COD < 125\ mg/l$ and the total suspended solid $TSS < 35\ mg/l$. These three quantities are defined below in terms of the state of the model.

The model used is based upon the Activated Sludge Model N[1] (ASM 1) from Henze et al. (1987). Then our biodegradation model consists of 12 state variables (Table 1): Actually, we consider only biodegradation, the state variables describing the total alkalinity being not included.

Insert table 1 about here

The three quality requirements characterizing the effluent are defined by:

$$\begin{aligned} BOD_5 &= 0.25(S_S + X_S + (1 - f_p)(X_{BH} + X_{BA})), \\ COD &= S_S + S_I + X_S + X_I + X_{BH} + X_{BA} + X_P, \\ TSS &= 0.75(X_S + X_I + X_{BH} + X_{BA} + X_P). \end{aligned} \tag{16}$$

Remark: 1. The stoichiometric and kinetic parameter values considered are listed in Tables 2 and 3. The complete set of equations and influent

conditions can be found on the International Water Association task group on benchmarking of control strategies for wastewater treatment plants website (http://www.benchmarkwwtp.org/, 2010).

2. Regarding the simplified model, in the paper, for the benefit of the reader, we provide **all explicit formulas and values** of the constants and kinetic functions.

Insert table 2 about here

Insert table 3 about here

The model assumptions are the following: - The reactor is well mixed, - the separation of liquid and solid phases is perfect and no reaction occurs in the settler, - the sum of all settler flowrates equals the settler influent flowrate. Our model is of the form $\dot{x} = f(x, u)$, where the control u consists of the state u_b of the turbines and the value Q^{in} of the influent average flow. The input u_b in (19) is a binary sequence switching between 0 and 1 and representing the state of turbines (off/on) that aerate the plant.

Natural coordinates are concentrations of the species, i.e. all components x_i of the state vector are the concentrations listed in Table 1. Each equation has the type of a material balance, including kinetic degradation, then the components f_i of the dynamics are as follows:

- For soluble components (i= 1, 2, 9, 10, 11)

$$f_i(x) = \frac{Q^{in}}{V}\left(x_i^{in} - x_i\right) + r_i(x) \tag{17}$$

- For particulate components (i= 3, 4, 5, 6, 7, 12)

$$f_i(x) = \frac{1}{V}\left[Q^{in}\left(x_i^{in} - x_i\right) + Q^{rs}\frac{Q^{in} - Q^w}{Q^{rs} + Q^w}x_i\right] + r_i(x) \tag{18}$$

- For dissolved oxygen concentration (i= 8)

$$f_8(x) = \frac{Q^{in}}{V}\left(x_8^{in} - x_8\right) + r_8(x) + u_b k_L a\,(S_O^{max} - S_O) \tag{19}$$

where $r_i(x)$, $i = 1, \cdots, 12$ are nonlinear functions not given here (see Henze et al. (1987)). They represent the apparent reaction rates depending on the kinetic rates of degradation of the components.

Remark: 3. The variables S_I, X_I and X_P, related with the equations corresponding to $i = 1,\ 3,\ 7$, do not appear in the other equations. Hence these variables are not observables, and we cannot do better for them than **simple prediction**. Therefore, pertinent dimension of the state space is $n = 9$.

The constant $k_L a$ is the oxygen transfer coefficient ($k_L a = 10\ h^{-1}$) and S_O^{max} is the dissolved oxygen saturation concentration ($S_O^{max} = 8\ mgl^{-1}$). The volume of the aeration tank is ($V = 6000\ m^3$). The settler is a cylindrical tank where the solids are either recirculated to the aeration tank ($Q^{rs} = 18446\ m^3 day^{-1}$) or extracted from the system ($Q^w = 385\ m^3 day^{-1}$).

We make here the reasonable assumption of three measurements only: S_O, S_{NO} and S_{NH}, located inside the aeration tank. Although the WWTP with these three outputs is observable, it is too complicated for our purpose. We use first a simplified model of lower dimension that has been developed in Chachuat et al. (2003).

5.1. The reduced model

The author in Chachuat et al. (2003) proceeds as follows: 1. He regroups the species S_S and X_S into a single one X_{COD} (COD for "chemical oxygen demand"), $X_{COD} = S_S + X_S$. 2. It is known that the dynamics of

X_{BH}, X_{BA}, X_{ND} are slow w.r.t. the other. Then, they are assumed to be constant. Hence the variables $\alpha_i,\ i = 1, .., 8$ defined below are constant. It is also commonly accepted that the ratios $\frac{X_{ND}}{X_S}$, $\frac{X_{COD}}{S_S}$, $\frac{X_{COD}}{X_S}$ vary slowly. As a consequence the variables α_9, K_{COD}, K_{ND} below are also assumed constant. Removing the three unobservable variables X_P, X_I, S_I leads to a simplified model with 5 state variables $S_O, S_{NO}, S_{NH}, X_{COD}, S_{ND}$ with the three observable variables S_O, S_{NO}, S_{NH}. All these simplifications provide the following reduced model:

$$\begin{aligned}\dot{S_O} &= \tfrac{Q^{in}}{V}\left(S_O^{in} - S_O\right) + \alpha_1 \tfrac{X_{COD}}{K_{COD}+X_{COD}} \\ &\cdot \tfrac{S_O}{K_{O,H}+S_O} + \widetilde{r_1}\left(y\right) + u_b k_L a\left(S_O^{max} - S_O\right)\end{aligned} \tag{20}$$

$$\begin{aligned}\dot{S_{NO}} &= \tfrac{Q^{in}}{V}\left(S_{NO}^{in} - S_{NO}\right) + \alpha_3 \tfrac{X_{COD}}{K_{COD}+X_{COD}} \\ &\cdot \tfrac{K_{O,H}}{K_{O,H}+S_O} \tfrac{S_{NO}}{K_{NO}+S_{NO}} + \widetilde{r_2}\left(y\right)\end{aligned} \tag{21}$$

$$\begin{aligned}\dot{S_{NH}} &= \tfrac{Q^{in}}{V}\left(S_{NH}^{in} - S_{NH}\right) + \alpha_5 \tfrac{X_{COD}}{K_{COD}+X_{COD}} \\ &\cdot \left(\tfrac{S_O}{K_{O,H}+S_O} + \eta_{NO,g} \tfrac{K_{O,H}}{K_{O,H}+S_O} \tfrac{S_{NO}}{K_{NO}+S_{NO}}\right) \\ &+ \widetilde{r_3}\left(y\right) + \alpha_6 S_{ND}\end{aligned} \tag{22}$$

$$\begin{aligned}\dot{X_{COD}} &= \tfrac{Q^{in}}{V}\left(X_{COD}^{in} - \tfrac{K_S}{K_{COD}} X_{COD}\right) \\ &+ \alpha_7 \tfrac{X_{COD}}{K_{COD}+X_{COD}} \left(\tfrac{S_O}{K_{O,H}+S_O}\right. \\ &\left. + \eta_{NO,g} \tfrac{K_{O,H}}{K_{O,H}+S_O} \tfrac{S_{NO}}{K_{NO}+S_{NO}}\right) + \alpha_8\end{aligned} \tag{23}$$

$$\begin{aligned}\dot{S_{ND}} &= \tfrac{Q^{in}}{V}\left(S_{ND}^{in} - S_{ND}\right) - \alpha_6 S_{ND} + \alpha_9 \\ &\cdot \tfrac{X_{COD}}{K_{ND}+X_{COD}} \left(\tfrac{S_O}{K_{O,H}+S_O} + \eta_{NO,h} \tfrac{K_{O,H}}{K_{O,H}+S_O}\right. \\ &\left. \cdot \tfrac{S_{NO}}{K_{NO}+S_{NO}}\right)\end{aligned} \tag{24}$$

The parameters α_1, α_2, α_3, α_4, α_5, α_6, α_7, α_8, α_9, K_{ND} and K_{COD} are defined as follows, their value is given in Table 4, the values of the influent concentrations being listed in Table 5.

$$\begin{aligned}
\alpha_1 &= -\tfrac{1-Y_H}{Y_H}\mu_H X_{B,H} \\
\alpha_2 &= -4.57\tfrac{\mu_A}{Y_A} X_{B,A} \\
\alpha_3 &= -\tfrac{1-Y_H}{2.86 Y_H}\mu_H X_{B,H}\eta_{NO,g} \\
\alpha_4 &= \tfrac{\mu_A}{Y_A} X_{B,A} \\
\alpha_5 &= -i_{XB}\mu_H X_{B,H} \\
\alpha_6 &= k_a X_{B,H} \\
\alpha_7 &= -\tfrac{1}{Y_H}\mu_H X_{B,H} \\
\alpha_8 &= (1-f_p)\left(b_H X_{B,H} + b_A X_{B,A}\right) \\
\alpha_9 &= k_h \tfrac{X_{ND}}{X_S} X_{B,H}
\end{aligned} \tag{25}$$

$$\begin{aligned}
K_{COD} &= K_S \tfrac{X_{COD}}{S_S} \\
K_{ND} &= K_X \tfrac{X_{COD}}{X_S} X_{B,H}
\end{aligned} \tag{26}$$

$$\begin{aligned}
\widetilde{r_1}(y) &= \alpha_2 \tfrac{S_{NH}}{K_{NH,A}+S_{NH}} \tfrac{S_O}{K_{O,A}+S_O} \\
\widetilde{r_2}(y) &= \alpha_4 \tfrac{S_{NH}}{K_{NH,A}+S_{NH}} \tfrac{S_O}{K_{O,A}+S_O} \\
\widetilde{r_3}(y) &= -\alpha_4 \tfrac{S_{NH}}{K_{NH,A}+S_{NH}} \tfrac{S_O}{K_{O,A}+S_O}
\end{aligned} \tag{27}$$

Insert table 4 about here

Insert table 5 about here

5.1.1. Observability analysis

For the simplified model (20 - 24), with outputs S_O, S_{NO}, S_{NH} the "practical" domain is $(\mathbb{R}_+)^5$, the positive orthant in $(\mathbb{R})^5$.

1. The points where S_O, S_{NO} are both zero may appear in practice, this is called "anaerobic behavior". This type of functioning remains nevertheless temporary and is not very frequent since the switch off period of the aerator is limited by the operating constraint $t_{max}^{off} = 120\ min$. In that case, the variable X_{COD} has no influence on the outputs. Therefore the system is not observable in any sense and there is nothing better to do than simple prediction.

2. On the subdomain $\mathfrak{D} \subset (\mathbb{R}_+)^5$, $\mathfrak{D} = \{S_O \neq 0 \text{ or } \ S_{NO} \neq 0\}$ it is easily computed that the system is uniformly observable and uniformly infinitesimally observable in the sense of Gauthier and Kupka (2001). This is reflected by the fact that the matrix $a_2(t)$ has rank two on $\mathfrak{D}$ (remember that a_2 is a function of t via is dependence on the output variables).

This is enough for the high-gain theory works, and in particular our adaptive algorithm developed in Boizot et al. (2010).

5.1.2. Change of variables

The change of variables Ψ that relates natural coordinates to observer coordinates is trivial: It consists of setting just

$$\widetilde{X_{COD}} = \frac{X_{COD}}{K_{COD} + X_{COD}}. \tag{28}$$

The state vector $x = (S_O\ S_{NO}\ S_{NH}\ X_{COD}\ S_{ND})'$ is changed for $\xi =$

$\left(S_O\ S_{NO}\ S_{NH}\ \widetilde{X_{COD}}\ S_{ND}\right)'$, therefore our system is almost naturally in observable coordinates. The inverse Jacobian is trivial to compute.

5.2. Observer for the complete model

The observability analysis of the full system with the estimate provided by the reduced observer is trivial (after forgetting about the unobservable variables S_I, X_I and X_P, see remark 3). It leads to similar conclusions of uniform observability and uniform infinitesimal observability.

In that case the state is 9-dimensional and the output is 6-dimensional: Actually the variables X_S, S_S that have been glued together in $X_{COD} = S_S + X_S$, can be splitted out from the reduced model. This is done using the previous assumption that K_{COD} is a constant (26):

$$\frac{X_{COD}}{S_S} = 1 + \frac{X_S}{S_S} = \frac{K_{COD}}{K_S}. \tag{29}$$

5.2.1. Change of variables

The change of variables ψ from natural to observable coordinates is trivial:
$x = (S_O\ S_{NO}\ S_{NH}\ S_S\ X_S\ S_{ND}\ X_{BH}\ X_{BA}\ X_{ND})'$ is changed for
$\xi = (S_O\ S_{NO}\ S_{NH}\ S_S\ X_S\ S_{ND}\ r_8\ r_9\ r_{11})'$.
Of course the functions $r_8\ r_9\ r_{11}$ are such that the change of variables is an embedding.

5.3. Choice of the parameters related to innovation

The choice of the parameters (θ_{max}, β, m, ΔT, λ, d) in the case of our application is given in Table 6.

Insert table 6 about here

Remember that the purpose of these parameters is to tune the way the high-gain evolves between 1 (EKF mode) and θ_{max} (HG mode). This choice has been obtained just by successive trials.

5.4. Conditions for a realistic simulation

5.4.1. Input concentrations

In order to perform realistic simulations, the influent concentrations (S_I^{in}, S_S^{in}, $\cdots$, X_{COD}^{in}) (typical values given in Table 5) cannot be considered as constant. We have modelled the variations of these concentrations by an additive noise. In practice, due the length of the feeding pipe (maybe several kilometers), these perturbations should appear rather slowly. However, we have willingly chosen fast dynamics for these noises. An illustrative example of these variations is shown on figure 3.

Insert figure 3 about here

5.4.2. Desadaptation of kinetic rates and stoichiometric coefficients

These parameters are not very well known in practice, and may be subject to large unexpected variation. We have considered simultaneously, for each reaction rate (theoretically given by Henze et al. (1987)) a periodic desadaptation of amplitude 20%. Moreover, these desadaptations are realized in a completely asynchrone way.

Here, we consider 3 periods over the 14 days under consideration, with a phase difference uniformly displayed over the 8 reaction rates.

These conditions of simulation 5.4.1 and 5.4.2 above are presumably worse than what may appear in practice.

6. Results

As commonly accepted, all simulations shown in this section are done with the outputs perturbed by a realistic additive Orstein-Uhlenbeck process. The alternative control u_b has been chosen as in practice: "On" during 15 minutes and "off" during 5 minutes. Our simulation file (dry weather) covers 14 days and the value of the input flow rate Q^{in} come from the benchmark file (http://www.benchmarkwwtp.org/, 2010).

To evaluate the performances of our observer on the WWTP, we compare a Luenberger observer, an ordinary EKF, and our adaptive HG-EKF. No comparison is shown with an ordinary HG-EKF (non adaptive): In that case the results are rather bad, the observer being very sensitive to noise. The averages and standard deviations are computed over the whole duration of 14 days. However the illustrative figures presented below show the 3 first days only, where the effect of the unknown initial conditions is significant.

The table 7 shows a clear improvement, for our adaptive HG observer.

Insert table 7 about here

6.1. Reconstruction of the variables X_I, S_I, X_P

As we said these unobservable variables are reconstructed by simple prediction. The results are shown in Table 8.

Insert table 8 about here

6.2. Effluent quality

To validate the method and estimate the effluent outputs, we simulate the complete settler as described in Takacs et al. (1991). This model simulates the solids profile throughout the settling column, including the underflow and effluent suspended solid concentrations. Comparisons of the three quality requirements with their estimates are presented in Table 9. In this table we show again the average and the standard deviation of the estimation error.

Insert table 9 about here

The figure 4 displays the output variables BOD_5, COD, TSS and their estimates, over 3 days. The effect of the high gain at the beginning of the response is very clear. The error really converges quickly to zero, which is not the case for the EKF, for which a significant error remains for long.

Insert figure 4 about here

7. Conclusion

The method proposed here for state reconstruction of a WWTP seems to be a real improvement with respect to classical methods. It is technically twofold: First the implementation of the adaptive HG-EKF is not too complicated due to the use of natural coordinates which simplifies hugely the computations. Second the use of a cascade observer also leads to reasonable computations for the complete model.

Note that here we have studied only the case of a 20 Celsius influent temperature (a summer scenario). The kinetic and stoichiometric parameters

of the models can be very different for a winter scenario. More generally a possible improvement could be a multi-model strategy taking into account the exterior temperature.

8. References

Alcaraz-Gonzalez, V., Harmand, J., Rapaport, A., Steyer, J.-P., Gonzalez-Alvarez, V., Pelayo-Ortiz, C., 2002. Software sensors for highly uncertain wwtps : a new approach based on interval observers. Water Research 36, 2515–2524.

Assis, A., Filho, R., 2000. Soft sensors development for on-line bioreactor state estimation. Computers and Chemical Engineering 24, 1099–1103.

Baras, J., Bensoussan, A., James, M., 1988. Dynamic observers as asymptotic limits of recursive filters: Special cases. SIAM Jounal on Applied Mathematics 48.5, 1147–1158.

Bastin, G., Dochain, D., 1990. On-line estimation and adaptive control of bioreactors. Elsevier Science Publishers.

Bastin, G., Impe, J. V., 1995. Nonlinear and adaptive control in biotechnology : A tutorial. European Journal of Control 1.1, 37–53.

Boizot, N., Busvelle, E., 2007. Adaptive-gain observers and applications in nonlinear observers and applications. In: Besanon, G. (Ed.), Lecture Notes in Control and In formation Sciences. Vol. 363. Springer-Verlag.

Boizot, N., Busvelle, E., Gauthier, J.-P., 2010. An adaptive high-gain observer for nonlinear systems. Automatica 46.9, 1483–1488.

Busvelle, E., Gauthier, J., 2003. On determining unknown functions in differential systems, with an application to biological reactors. ESAIM : Control, Optimisation abd Calculus of Variations 9, 509–551.

Busvelle, E., Gauthier, J., 2005. Observation and identification tools for nonlinear systems : application to a fluid catalytic cracker. International journal of control 78.3, 208–234.

Chachuat, B., Roche, N., Latifi, M., 2003. Reduction of the asm1 model for optimal control of small-size activated sludge treatment plants. Journal of Water Science / Revue des Sciences de l'eau 16.1, 05–26.

Dochain, D., 2008. Bioprocess control. Vol. ISBN 9781848210257. ISTE.

Gauthier, J., Hammouri, H., Othman, S., 1992. A simple observer for nonlinear systems. application to bioreactors. IEEE Transactions on Automatic Control 37.6, 875–880.

Gauthier, J.-P., Kupka, I., 2001. Deterministic Observation Theory and Applications. Cambridge university Press, Cambridge.

Henze, M., Grady, C., Gujer, W., Marais, G., Matsuo, T., 1987. Activated sludge model n1. In: IAWQ (Ed.), Technical Report 1. London.

http://www.benchmarkwwtp.org/, 2010.

Nejjari, F., Puig, V., Giancristofaro, L., Koehler, S., 2008. Extended luenberger observer-based fault detection for an activated sludge process. Proceedings of the 17th World Congress The International Federation of Automatic Control, Seoul, Korea, 9725–9730.

Rapaport, A., Dochain, D., 2005. Interval observers for biochemical processes with uncertain kinetics and inputs. Mathematical biosciences 193, 235–253.

Sotomayor, O., Park, S., Garcia, C., 2002. Software sensor for on-line estimation of the microbial activity in activated sludge systems. ISA Transactions 41, 127–143.

Takacs, I., Patry, G., Nolasco, D., 1991. A dynamic model of the clarification thickening process. Water Research 25.10, 1263–1271.

A. Change of variables in the HG-EKF

We do the computations in the case of our two applications only, that have special features w.r.t the general cases where the theory applies:

1. The change of variables is of the form $x = \Phi(\xi)$, where x is the original coordinate and ξ is the "observable coordinate". In general it is not the case, but $\xi = \psi(x, u)$.

2. The output consists of the first state coordinates i.e. $C = (I_d, 0)$, $y = Cx = C\xi$, $CT\Phi(\xi) = C$.

Also, in the computations below, equations are $\dot{x} = f(x, u(t))$ and $\dot{\xi} = F(\xi, u(t))$. But we omit the dependence in t and we use $\dot{x} = f(x), \dot{\xi} = F(\xi)$. This has no consequence in the computations. Also, the fact that Q_θ, R_θ depend on θ that itself depends on t has no consequence. In fact, the matrix $A(t)$ above depends on t via a dependence on the outputs S_O, S_{NO} and S_{NH}.

We set $\dot{\xi} = F(\xi, t)$, $x = \Phi(\xi)$, $\hat{x} = \Phi\left(\hat{\xi}\right)$, then, $T\Phi \circ \Phi^{-1}(x) F(\Phi^{-1}(x), t) = f(x, t)$.

Or, dropping t from now on: $f \circ \Phi(\xi) = T\Phi(\xi) F(\xi)$.

It follows that:

$Tf\left(\Phi\left(\xi\right)\right)T\Phi\left(\xi\right)=D^{2}\Phi\left(\xi\right)\left(F\left(\xi\right)\right)+T\Phi\left(\xi\right)TF\left(\xi\right).$

Hence:

$$\begin{array}{l} Tf\left(x\right)=D^{2}\Phi\left(\xi\right)\left\{F\left(\xi\right)\right\}T\Phi\left(\xi\right)^{-1} \\ +T\Phi\left(\xi\right)TF\left(\xi\right)T\Phi\left(\xi\right)^{-1}\ if\ x=\Phi\left(\xi\right). \end{array} \tag{30}$$

The equations of the HG-EKF are:

$$\begin{array}{l} \dot{\hat{\xi}}=F\left(\hat{\xi}\right)+PC^{'}R_{\theta}^{-1}\left(y-C\hat{\xi}\right) \\ \dot{\hat{x}}=T\Phi\left(\hat{\xi}\right)\dot{\hat{\xi}}=T\Phi\left(\hat{\xi}\right)F\left(\hat{\xi}\right) \\ +T\Phi\left(\hat{\xi}\right)P\ T\Phi\left(\hat{\xi}\right)^{'}\left(T\Phi\left(\hat{\xi}\right)^{'}\right)^{-1}\cdot C^{'}R_{\theta}^{-1}\left(y-C\hat{\xi}\right). \end{array} \tag{31}$$

Setting $p=T\Phi\left(\hat{\xi}\right)P\ T\Phi\left(\hat{\xi}\right)^{'}$,

$$\dot{\hat{x}}=f\left(\hat{x}\right)+p\ C^{'}R_{\theta}^{-1}\left(y-C\hat{\xi}\right). \tag{32}$$

The equation for P is:

$$\dot{P}=TF\left(\hat{\xi}\right)P+P\ TF\left(\hat{\xi}\right)^{'}+Q_{\theta}-PC^{'}R_{\theta}^{-1}CP, \tag{33}$$

which produces:

$$\dot{p}=T\Phi\left(\hat{\xi}\right)\dot{P}\ T\Phi\left(\hat{\xi}\right)^{'}+\overbrace{T\Phi\left(\hat{\xi}\right)}^{\bullet}P\ T\Phi\left(\hat{\xi}\right)^{'}+T\Phi\left(\hat{\xi}\right)P\ \overbrace{T\Phi\left(\hat{\xi}\right)}^{\bullet^{'}}, \tag{34}$$

$$
\begin{aligned}
&\dot{p} = T\Phi\left(\hat{\xi}\right) TF\left(\hat{\xi}\right) T\Phi\left(\hat{\xi}\right)^{-1} p \\
&+p\left(T\Phi\left(\hat{\xi}\right) TF\left(\hat{\xi}\right) T\Phi\left(\hat{\xi}\right)^{-1}\right)' \\
&+T\Phi\left(\hat{\xi}\right) Q_\theta T\Phi\left(\hat{\xi}\right)' - pC' R_\theta^{-1} Cp \\
&+\overbrace{T\Phi\left(\hat{\xi}\right)}^{\bullet} P\, T\Phi\left(\hat{\xi}\right)' + T\Phi\left(\hat{\xi}\right) P\, \overbrace{T\Phi\left(\hat{\xi}\right)}^{\bullet}{}'.
\end{aligned}
\tag{35}
$$

By (30):

$$
\begin{aligned}
&\dot{p} = \left(Tf\left(\hat{\xi}\right) - D^2\Phi\left(\hat{\xi}\right)\left\{F\left(\hat{\xi}\right)\right\} T\Phi\left(\hat{\xi}\right)^{-1}\right) p \\
&+p\left(Tf\left(\hat{\xi}\right) - D^2\Phi\left(\hat{\xi}\right)\left\{F\left(\hat{\xi}\right)\right\} T\Phi\left(\hat{\xi}\right)^{-1}\right)' \\
&+q - pC^T R_\theta^{-1} Cp \\
&+\overbrace{T\Phi\left(\hat{\xi}\right)}^{\bullet} P\, T\Phi\left(\hat{\xi}\right)' + T\Phi\left(\hat{\xi}\right) P\, \overbrace{T\Phi\left(\hat{\xi}\right)}^{\bullet}{}',
\end{aligned}
\tag{36}
$$

where $q = T\Phi\left(\hat{\xi}\right) Q_\theta T\Phi\left(\hat{\xi}\right)'$, or:

$$
\begin{aligned}
&\dot{p} = Tf\left(\hat{x}\right) p + pTF\left(\hat{x}\right)' + q - pC^T R_\theta^{-1} Cp \\
&-D^2\Phi\left(\hat{\xi}\right)\left\{F\left(\hat{\xi}\right)\right\} T\Phi\left(\hat{\xi}\right)^{-1} p \\
&-p\left(D^2\Phi\left(\hat{\xi}\right)\left\{F\left(\hat{\xi}\right)\right\} T\Phi\left(\hat{\xi}\right)^{-1}\right)' \\
&+\overbrace{T\Phi\left(\hat{\xi}\right)}^{\bullet} T\Phi\left(\hat{\xi}\right)^{-1} p + p\left(T\Phi\left(\hat{\xi}\right)^{-1}\right)' \overbrace{T\Phi\left(\hat{\xi}\right)}^{\bullet}{}'.
\end{aligned}
\tag{37}
$$

$$\begin{cases} \dot{p} = (I) + (II) + (III), \\ (I) = Tf(\hat{x})\, p + p\,(TF(\hat{x}))' \\ +q - pC^T R_\theta^{-1} Cp, \\ (II) = \left(\overbrace{T\Phi\left(\hat{\xi}\right)}^{\bullet} - D^2\Phi\left(\hat{\xi}\right)\left\{F\left(\hat{\xi}\right)\right\} \right) \\ \cdot T\Phi\left(\hat{\xi}\right)^{-1} p, \\ (III) = (II)'. \end{cases} \tag{38}$$

Now, let us compute $\overbrace{T\Phi\left(\hat{\xi}\right)}^{\bullet}$:

$$\begin{aligned} &\overbrace{T\Phi\left(\hat{\xi}\right)}^{\bullet} = D^2\Phi\left(\hat{\xi}\right)\left\{\dot{\hat{\xi}}\right\} \\ &= D^2\Phi\left(\hat{\xi}\right)\left\{F\left(\hat{\xi}\right) + PC' R_\theta^{-1}\left(y - C\hat{\xi}\right)\right\}. \end{aligned} \tag{39}$$

We use now the following formula, just coming from the fact that $0 = T^2\left(\Phi^{-1} \circ \Phi(\xi)\right)$:

$$\begin{aligned} &0 = T^2\Phi^{-1} \circ \Phi(\xi)\left(T\Phi(\xi)\, u, T\Phi(\xi)\, v\right) \\ &+T\Phi^{-1}(x)\, T^2\Phi(\xi)(u, v). \end{aligned} \tag{40}$$

455 Or

$$\begin{aligned} &D^2\Phi(\xi)\{u\} = -T\Phi(x)\, D^2\Phi^{-1}(x) \\ &\left\{T\Phi^{-1}(x)^{-1} u\right\} T\Phi(\xi). \end{aligned} \tag{41}$$

Putting (39) in (38) gives:

$$\begin{aligned} &(II) = D^2\Phi(\xi)\left\{PC' R_\theta^{-1}\left(y - C\hat{\xi}\right)\right\} \\ &\cdot T\Phi\left(\hat{\xi}\right)^{-1} p, \end{aligned} \tag{42}$$

and using (41),

$$\begin{array}{l}(II) = -T\Phi\left(\hat{x}\right) D^2\Phi^{-1}\left(\hat{x}\right) \\ \left\{T\Phi\left(\hat{\xi}\right) P\ T\Phi\left(\hat{\xi}\right)^{'} C^{'} R_{\theta}^{-1}\left(y - C\hat{x}\right)\right\} p,\end{array} \tag{43}$$

$$(II) = -T\Phi\left(\hat{x}\right) D^2\Phi^{-1}\left(\hat{x}\right)\left\{pC^{'} R_{\theta}^{-1}\left(y - C\hat{x}\right)\right\} p. \tag{44}$$

Going back to (38), we get:

$$\begin{array}{l}\dot{p} = Tf\left(\hat{x}\right) p + pTf\left(\hat{x}\right)^{'} + q - pC^T R_{\theta}^{-1} Cp \\ +T\Phi\left(\hat{x}\right) D^2\Phi^{-1}\left(\hat{x}\right)\left\{pC^{'} R_{\theta}^{-1}\left(C\hat{x} - y\right)\right\} p \\ +p\left(D^2\Phi^{-1}\left(\hat{x}\right)\left\{pC^{'} R_{\theta}^{-1}\left(C\hat{x} - y\right)\right\}\right)^{'} T\Phi\left(\hat{x}\right)^{'}.\end{array} \tag{45}$$

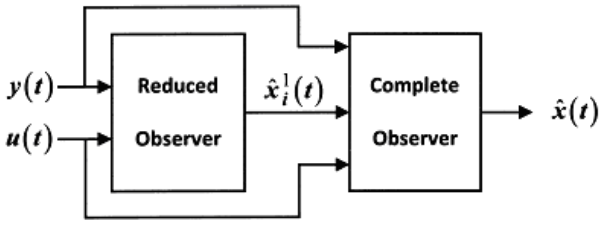

Figure 1: The cascade observer

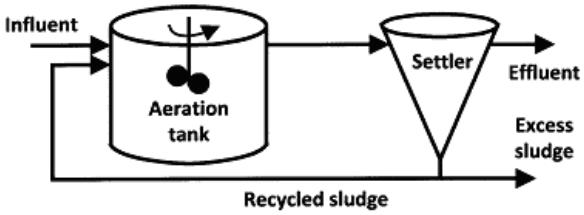

Figure 2: Wastewater treatment plant

Definition	Notation
1. Soluble inert organic matter ($g\,COD.m^{-3}$)	S_I
2. Readily biodegradable substrate ($g\,COD.m^{-3}$)	S_S
3. Particulate inert organic matter ($g\,COD.m^{-3}$)	X_I
4. Slowly biodegradable substrate ($g\,COD.m^{-3}$)	X_S
5. Active heterotrophic biomass ($g\,COD.m^{-3}$)	$X_{B,H}$
6. Active autotrophic biomass ($g\,COD.m^{-3}$)	$X_{B,A}$
7. Particulate products arising from biomass decay ($g\,COD.m^{-3}$)	X_P
8. Oxygen ($g\,COD.m^{-3}$)	S_O
9. Nitrate and nitrite nitrogen ($g\,N.m^{-3}$)	S_{NO}
10. $NH_4^+ + NH_3$ nitrogen ($g\,N.m^{-3}$)	S_{NH}
11. Soluble biodegradable organic nitrogen ($g\,N.m^{-3}$)	S_{ND}
12. Particulate biodegradable organic nitrogen ($g\,N.m^{-3}$)	X_{ND}

Table 1: List of variables

Parameter	Unit	Value
Y_A	$g\ cell\ COD\ formed$ $(g\ N\ oxidized)^{-1}$	0.24
Y_H	$g\ cell\ COD\ formed$ $(g\ COD\ oxidized)^{-1}$	0.67
f_p	$dimensionless$	0.08
i_{XB}	$g\ N\ (g\ COD)^{-1}$ $in\ biomass$	0.08
i_{XP}	$g\ N\ (g\ COD)^{-1}$ $in\ particulate\ products$	0.06

Table 2: Stoichiometric parameters.

Parameter	Unit	Value
μ_H	d^{-1}	4.0
K_S	$g\ COD\ m^{-3}$	10.0
$K_{O,H}$	$g\ COD\ m^{-3}$	0.2
K_{NO}	$g\ NO_3 - N\ m^{-3}$	0.5
b_H	d^{-1}	0.3
$\eta_{NO,g}$	$dimensionless$	0.8
$\eta_{NO,h}$	$dimensionless$	0.8
k_h	$(g\ cell\ COD\ d)^{-1}$	3.0
K_X	$(g\ cell\ COD)^{-1}$	0.1
μ_A	d^{-1}	0.5
$K_{NH,A}$	$g\ NH_3 - N\ m^{-3}$	1.0
b_A	d^{-1}	0.05
$K_{O,A}$	$g\ COD\ m^{-3}$	0.4
k_a	$m^3\ (g\ COD\ d)^{-1}$	0.05

Table 3: Kinetic parameters.

Coefficient	Value
α_1	- 5892
α_2	- 875
α_3	- 1648
α_4	191
α_5	- 957
α_6	150
α_7	- 17855
α_8	830
α_9	561
K_{COD}	574
K_{ND}	296

Table 4: Constant coefficients.

Concentration	Value
S_I^{in}	30 $g\ COD\ m^{-3}$
S_S^{in}	69.5 $g\ COD\ m^{-3}$
X_I^{in}	51.2 $g\ COD\ m^{-3}$
X_S^{in}	202.32 $g\ COD\ m^{-3}$
X_{BH}^{in}	28.17 $g\ COD\ m^{-3}$
X_{BA}^{in}	0 $g\ COD\ m^{-3}$
X_P^{in}	0 $g\ COD\ m^{-3}$
S_O^{in}	0 $g\ COD\ m^{-3}$
S_{NO}^{in}	0 $g\ COD\ m^{-3}$
S_{NH}^{in}	31.56 $g\ COD\ m^{-3}$
S_{ND}^{in}	6.95 $g\ COD\ m^{-3}$
X_{ND}^{in}	10.59 $g\ COD\ m^{-3}$
X_{COD}^{in}	271.82 $g\ COD\ m^{-3}$

Table 5: Influent concentrations.

Parameter	value of the reduced observer	value of the complete observer
θ_{max}	20	10
β	$1664\frac{\pi}{e}$	$1664\frac{\pi}{e}$
m	2	40
ΔT	0.01	0.01
λ	200	200
d	0.1	0.1

Table 6: Parameters for the adaptation.

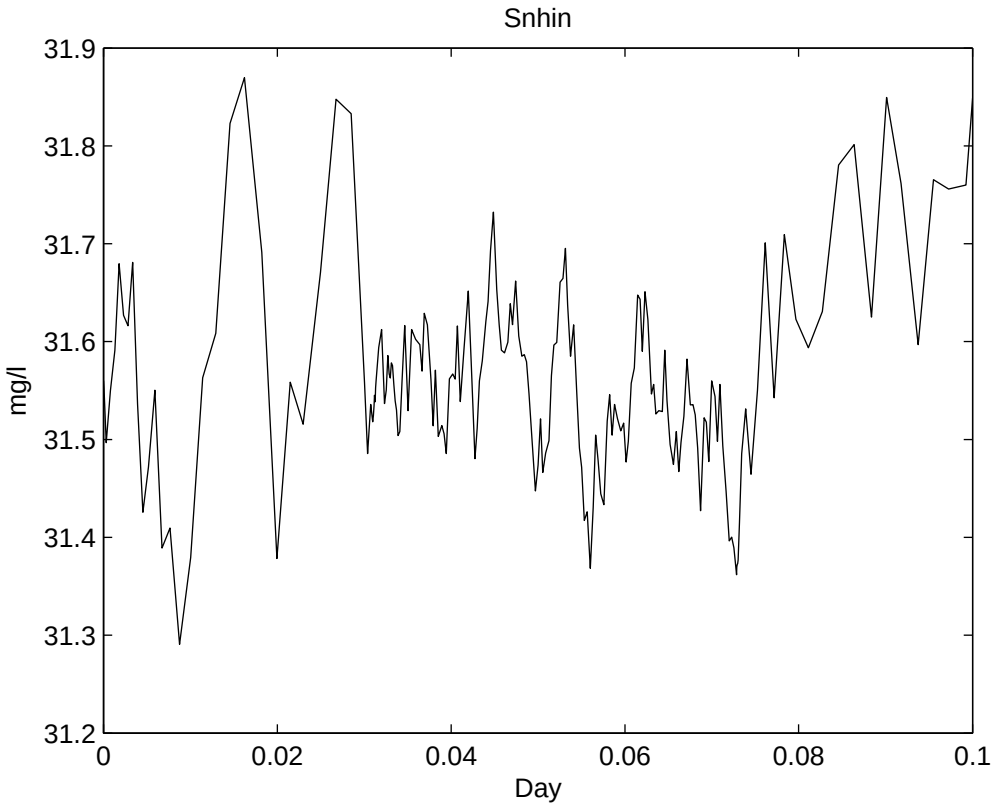

Figure 3: Variation of S_{NH}^{in}

Variable	Luenberger		EKF		HG-EKF		Range
	m	σ	m	σ	m	σ	
S_{ND}	-0.02	0.07	-0.02	0.07	-0.01	0.08	[0.5 - 1.2]
S_S	-0.03	0.11	-0.03	0.11	-0.02	0.10	[0.6 - 1.7]
X_S	0.30	7.85	0.28	7.86	-0.21	7.59	[38.3 - 110.0]
X_{BH}	96.17	81.39	96.68	81.29	41.64	85.52	[2635.3 - 3670.7]
X_{BA}	-8.29	4.50	-7.20	4.41	-5.89	3.14	[75.0 - 154.2]
X_{ND}	0.02	0.61	0.02	0.61	-0.02	0.60	[2.7 - 7.0]

Table 7: Comparisons between Luenberger, EKF and adaptive HG-EKF.

Variable	Luenberger		EKF		HG-EKF		Range
	m	σ	m	σ	m	σ	
S_I	-0.03	0.12	-0.03	0.12	-0.03	0.12	[29.9 - 30.1]
X_I	3.93	1.89	3.94	1.88	3.76	1.84	[1224.7 - 1259.2]
X_P	28.48	8.42	28.51	8.40	20.29	7.82	[270.0 - 510.4]

Table 8: Comparisons between Luenberger, EKF and adaptive HG-EKF.

Quality requirements	Luenberger		EKF		HG-EKF		Range
	m	σ	m	σ	m	σ	
BOD_5	0.04	0.04	0.04	0.04	0.01	0.04	[0 - 2.2]
COD	0.22	0.15	0.22	0.15	0.09	0.15	[0 - 30.1]
TSS	0.18	0.13	0.19	0.13	0.09	0.10	[0 - 9.2]

Table 9: Quality requirements.

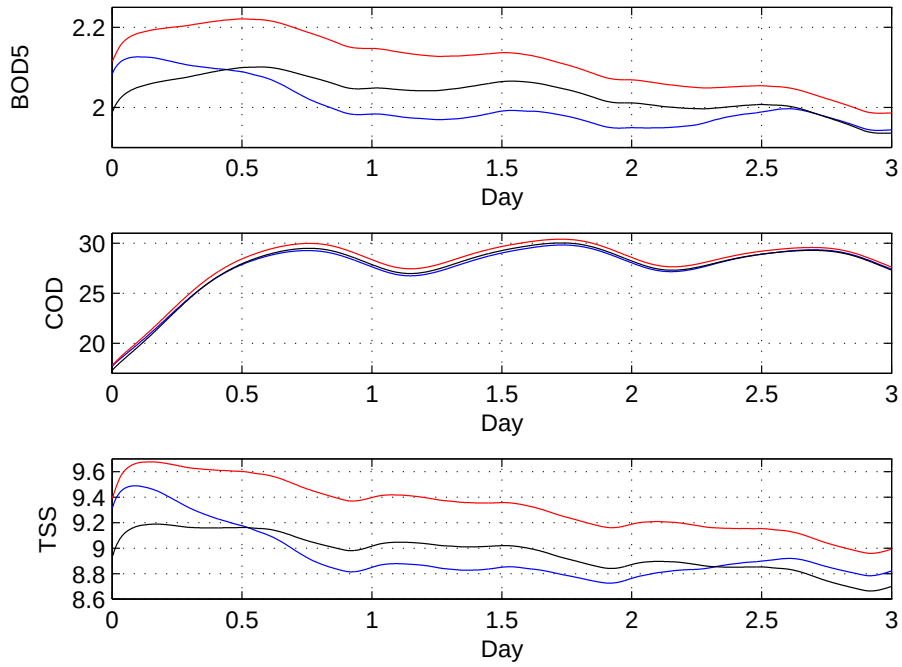

Figure 4: Effluent quality (black: model - red : EKF observer - blue: HG-EKF observer)